Structure and dynamics of the lipid modifications of a transmembrane α-helical peptide determined by ^{2}H solid-state NMR spectroscopy

Anja Penk [a], Matthias Müller [a], Holger A. Scheidt [a], Dieter Langosch [b,c], Daniel Huster [a,*]

[a] Institute of Medical Physics and Biophysics, University of Leipzig, Härtelstr. 16-18, D-04107 Leipzig, Germany
[b] Lehrstuhl für Chemie der Biopolymere, Technische Universität München, Weihenstephaner Berg 3, D-85354 Freising, Germany
[c] Munich Center For Integrated Protein Science (CIPS^M), Munich, Germany

ARTICLE INFO

ABSTRACT

The fusion of biological membranes is mediated by integral membrane proteins with α-helical transmembrane segments. Additionally, those proteins are often modified by the covalent attachment of hydrocarbon chains. Previously, a series of *de novo* designed α-helical peptides with mixed Leu/Val sequences was presented, mimicking fusiogenically active transmembrane segments in model membranes (Hofmann et al., Proc. Natl. Acad. Sci. USA 101 (2004) 14776–14781). From this series, we have investigated the peptide LV16 (KKKW LVLV LVLV LVLV LVLV KKK), which was synthesized featuring either a free N-terminus or a saturated N-acylation of 2, 8, 12, or 16 carbons. We used ^{2}H and ^{31}P NMR spectroscopy to investigate the structure and dynamics of those peptide lipid modifications in POPC and DLPC bilayers and compared them to the hydrocarbon chains of the surrounding membrane. Except for the C2 chain, all peptide acyl chains were found to insert well into the membrane. This can be explained by the high local lipid concentrations the N-terminal lipid chains experience. Further, the insertion of these peptides did not influence the membrane structure and dynamics as seen from the ^{2}H and ^{31}P NMR data. In spite of the fact that the longer acyl chains insert into the membrane, they do not adapt their lengths to the thickness of the bilayer. Even the C16 lipid chain on the peptide, which could match the length of the POPC palmitoyl chain, exhibited lower order parameters in the upper chain, which get closer and finally reach similar values in the lower chain region. ^{2}H NMR square law plots reveal motions of slightly larger amplitudes for the peptide lipid chains compared to the surrounding phospholipids. In spite of the significantly different chain lengths of the acylations, the fraction of gauche defects in the inserted chains is constant.

1. Introduction

Fusion of biological membranes is an intensely investigated yet very complex process mediated by integral membrane proteins, e.g. the SNARE machinery operating within the secretory pathway [1]. Although the general patterns underlying fusion events are known, no complete biophysical picture of the cellular fusion mechanism can be sketched. Therefore, model systems still provide valuable information about molecular details of the fusion event. Several studies have highlighted the influence of transmembrane domains on fusion proteins in this process [2]. For instance, *de novo* designed model peptides, like KALR [3] or LV peptides [4], which mimic the transmembrane domains of fusion proteins, have been shown to promote *in vitro* fusion and used as simplified models to systematically investigate structure/function relationships without the influence of membrane-extrinsic domains. Such low-complexity model

systems allow to study one specific aspect of a complicated biological problem with atomistic detail. LV peptides mimic a basic aspect of transmembrane domains of natural fusion proteins in that they fuse model membranes, presumably by increasing the likelihood that randomly colliding liposomes undergo fusion [5]. Further, studying a series of variants indicated the importance of helix-destabilizing residues for backbone dynamics and fusogenicity [4].

LV peptides consist of a hydrophobic core, comprising leucine (L) and valine (V) residues in varying ratios as the β-branched amino acids Ile and Val are overrepresented in SNARE transmembrane domains [6], which are flanked by three lysines (K) on each side and completed by tryptophan (W) at the N-terminal interface between the K and the L/V residues. The secondary structure of reconstituted LV peptides as well as their fusion-promoting effect has been investigated as a function of the length of the hydrophobic core, the L/V ratio, the insertion of helix breakers [7], and the influence of charge [8]. Furthermore, the interaction of the peptides with membranes was studied [9]. LV peptides can give rise to pronounced macroscopic lipid rearrangements. Specifically, the more fusogenic variants induce unaligned lipid phase and phase

separation [9]. It appears that enhanced dynamics of the helix backbone in terms of local and transient unfolding of the chain may affect the membrane structure and thereby favorably influence the fusion event [4].

Another aspect of fusion proteins that has rarely been investigated is the fact that these proteins often carry covalently attached lipid chains [10,11]. Lipidation is known as a commonly occurring membrane anchor in many membrane-associated proteins and a number of structural motifs such as isoprenylation, myristoylation, or palmitoylation have evolved [12]. Research on model peptides of varying origins has indicated that only the concerted action of at least two lipid modifications provides stable membrane insertion [13,14]. However, lipid modifications on membrane-spanning fusion proteins should not be required to anchor these molecules to the membrane. Rather, a different task could be envisioned, for instance, a fusion-promoting function. Recent molecular dynamics simulations have shown that stalk formation is initiated by a localized hydrophobic contact between the opposing membranes, formed by fully or partially splayed lipids [15]. This agrees with the experimental finding that lipid tail-to-head contacts are frequently observed in membranes [16,17]. A possible involvement of backfolded and thus water exposed protein lipid modifications in membrane fusion events appears particularly interesting. Thus, the lipid chain of a fusion protein could indeed be highly flexible and partially water exposed, such that it could insert into the opposing membrane during fusion. This would facilitate the molecular contact between these membranes and the protein lipid chain would act as the splayed lipid that initiates fusion [15].

In contrast to this rationale, experimental studies of N-terminally lipidated LV16 peptides revealed a decrease in fusogenic activity, which was more pronounced for the longer lipid modifications [18]. However, the lipid modifications appeared to stabilize global helicity without affecting backbone dynamics [19]. This may suggest that the lipid modification of LV16 would not promote the approach of opposing membranes, but influence fusion by a stabilization of the transmembrane domains. Nevertheless, an influence of acylation on the hemifusion-to-fusion transition has been reported for viral envelope proteins [20] and other fusion proteins [21–23].

To understand the role of covalent lipid chains in the process of fusion structural and dynamical aspects of the lipid modifications of fusion proteins or their transmembrane domains are essential. Although lipid modification is relevant for up to 10% of all cellular proteins, there is only little biophysical data available. In particular, the structural aspects [12] of lipid modifications along with the thermodynamics of membrane insertion [13,24] are of interest for the understanding of their role in biological function. Since membrane-inserted protein lipid chains are composed of the same atomic groups as the chains of the phospholipids, spectroscopic techniques that are sensitive to the hydrogen/deuterium isotope effect, such as neutron scattering or FTIR spectroscopy, are particularly useful [25]. In addition, ^{2}H NMR has proved very useful to analyze the structure and dynamics of lipid-modified peptides and proteins [12,26–28]. These methods allow to determine segment-specific chain order parameters [29,30], which can be converted into geometrical parameters such as lipid chain length and area per molecule [31]. Further, dynamic aspects of lipid chains can be assessed by measurement of nuclear relaxation rates and their analyses by motion models [27,32].

Here, we have studied transmembrane LV16 peptides that were N-terminally acylated with saturated C2, C8, C12, and C16 chains, respectively. In contrast to previous findings on other lipid-modified proteins [28], we find that the peptide lipid chains are much less influenced by the host membrane and show properties that are largely independent of those of the surrounding phospholipids. This could indeed support a structure stabilizing function of these chains.

2. Materials and methods

2.1. Materials

1-Palmitoyl-2-oleoyl-*sn*-glycero-3-phosphocholine (POPC) and 1,2-dilauroyl-*sn*-glycero-3-phosphocholine (DLPC), as well as the analogs of these phospholipids with perdeuterated acyl chains, POPC-d_{31} (1-palmitoyl(d_{31})-2-oleoyl-*sn*-glycero-3-phosphocholine) and DLPC-d_{46} (1,2-dilauroyl(d_{46})-*sn*-glycero-3-phosphocholine), were obtained from Avanti Polar Lipids (Alabaster, AL) and used without further purification.

The LV16 peptides (sequence: acyl-KKKWL VLVLV LVLVL VLVLV KKK) with (LV16ac) or without (LV16) a covalently attached N-terminal saturated acyl chain were synthesized by standard Fmoc chemistry. Either protonated or perdeuterated acyl chains containing 2, 8, 12, or 16 carbons were used. Synthesis products were purified to >95% by HPLC as confirmed by mass spectrometry.

2.2. Sample preparation

Lipids prepared in chloroform were combined with peptides solved in 2,2,2-trifluoroethanol (TFE) at a molar ratio of 30:1 (the lipid to peptide mixing ratio considers the mass of lyophilized peptide powder used, which also includes approximately 30% counterions, TFA, etc.), diluted with cyclohexane, and vortexed, and after freezing in liquid nitrogen, samples were lyophilized overnight. Afterwards, samples were dissolved in cyclohexane and lyophilized overnight for a second time to obtain a fluffy powder. Multilamellar proteolipo-somes were prepared by hydrating the sample to a water content of 50 wt.% with aqueous buffer (150 mM NaCl, 0.1 mM EDTA 25 mM Tris–HCl, pH 7.4) Several freeze–thaw cycles interrupted by gentle centrifugation were performed to homogenize the sample.

2.3. Deuterium solid-state NMR spectroscopy

^{2}H NMR spectra were acquired on a Bruker Avance 750 MHz NMR spectrometer (Bruker Biospin GmbH, Rheinstetten, Germany) operating at a resonance frequency of 115.1 MHz for ^{2}H. A single-channel solids probe equipped with a 5 mm solenoid coil was used. The ^{2}H NMR spectra were accumulated with a spectral width of ± 250 kHz using quadrature detection. A phase-cycled quadrupolar echo sequence was used [33]. The length of a 90° pulse varied from 2.2 to 3.9 μs, and a relaxation delay of 1 s was applied. For the measurement of the T_1 spin-lattice relaxation times, a phase-cycled inversion recovery quadrupolar echo pulse sequence with 11 time delays between 1 ms and 2.5 s was used. The relaxation delay was 2.5 s; all other parameters were identical as for recording the ^{2}H NMR spectra. All measurements were conducted at a temperature of 310 K.

The ^{2}H NMR powder spectra were de-Paked using the algorithm of Mc Cabe and Wassall [34] and the order parameter profiles of the lipid chains were determined by a numerical spectral fitting procedure from the observed quadrupolar splitting in the dePaked spectra $\Delta\nu_Q(n)$:

$$\Delta\nu_Q(n) = \frac{3}{2}\frac{e^2qQ}{h}S(n),$$

where e^2qQ/h is the quadrupolar coupling constant (167 kHz for ^{2}H in a C-^{2}H bond) and $S(n)$ the chain order parameter for the nth carbon position in the chain.

The length of the acyl chain L_c^* (also referred to as chain extent), the mean interfacial area (A) and the hydrocarbon thickness (D_c) were calculated according to the mean torque model [26,31]. For a given lipid chain with a specific length, the number of gauche conformers can be estimated by subtracting the measured chain length from the length of the all trans chain (assuming a projected

chain length of 1.27 Å per C-C bond). Assuming that one gauche defect reduces the chain length by 1.1 Å [35] allows to calculate the number of gauche defects per chain.

For the analysis of the relaxation measurements, the line shape of the ^{2}H NMR powder spectra with the longest delay time was simulated by a superposition of the respective number of Pake doublets (for the CH$_2$ and CH$_3$ groups) using Mathcad 2001 (MathSoft Engineering & Education, Inc., Cambridge, MA). Then, the program determines the relaxation time for each individual Pake doublet by a fitting procedure that calculates the ^{2}H NMR spectrum for each inversion recovery delay and compares it with the experimental spectrum.

2.4. ^{31}P NMR measurements

Static ^{31}P NMR spectra were measured on a Bruker DRX 600 NMR spectrometer operating at a resonance frequency of 242.8 MHz for ^{31}P using a Hahn-echo pulse sequence. A ^{31}P 90° pulse length of 11 μs, a Hahn-echo delay of 50 μs, a spectral width of 100 kHz, and a recycle delay of 2.5 s were used. Continuous-wave low power proton decoupling was applied during signal acquisition. All measurements were conducted at a temperature of 310 K. The measured NMR spectra were simulated using a program written in Mathcad 2001 to obtain the chemical shift anisotropy.

3. Results

3.1. LV16ac in POPC membranes

First, acylated LV16ac peptides were investigated in zwitterionic POPC membranes. By switching the ^{2}H label between the phospholipid and the peptide lipid chains, independent information about the structure and dynamics of those chains could be gathered. For each lipid-modified peptide, ^{2}H NMR spectra of (i) pure POPC-d_{31}, (ii) POPC-d_{31} in the presence of the LV16ac peptide with protonated lipid chain, and (iii) POPC in the presence of the LV16ac-d_x ($x = 3$, 15, 23, or 31) peptide with perdeuterated lipid chain were recorded. In all samples including peptide, the peptide to lipid molar ratio was 1:30.

This combination of samples allows comparing structural and dynamic information of the lipid and peptide chains as well as determining the influence of the peptide on the host POPC membrane.

The ^{2}H NMR spectra of POPC-d_{31} in the absence and in the presence of LV16ac, as well as of the acyl chains of LV16ac8-d_{15}, LV16ac12-d_{23} and LV16ac16-d_{31} in a protonated POPC membrane show a typical well resolved powder spectrum. Representative ^{2}H NMR spectra are shown in Fig. 1. The ^{2}H NMR spectra of POPC-d_{31} in the presence and in the absence of LV16ac are virtually indistinguishable. In contrast, very pronounced differences are observed for the ^{2}H NMR spectra of the acylated peptides. The ^{2}H NMR spectrum of LV16ac2-d_3 with a C2 lipid chain is dominated by an isotropic line. Some very weak quadrupolar splittings can be observed on the foot of this line when it is magnified, which accounts for ~8% of the spectral intensity. This represents a minor fraction of membrane-inserted C2 chain while the large majority of this chain is isotropically mobile in the aqueous phase. LV16ac peptides carrying C8, C12, or C16 lipid chains gave rise to ^{2}H NMR spectra that can be described by a superposition of Pake doublets with varying quadrupolar splitting. Such spectra are characteristic of fully membrane-inserted lipid chains. Interestingly, no isotropic signals are observed in these spectra confirming that the peptide lipid chains are fully inserted into the membrane.

From these ^{2}H NMR spectra, order parameter profiles can be calculated and are shown in Fig. 2A (the typical error for the order parameter determination is smaller than the symbol size). The order parameter plots for POPC-d_{31} in the presence of the LV16ac peptides are virtually identical and only slightly larger than POPC-d_{31} in the absence of the transmembrane α-helix. This indicates that the transmembrane peptide does not influence the structure and dynamics of the lipid matrix. This further suggests that peptide and membrane have very similar hydrophobic thicknesses. With 17 hydrophobic residues, an α-helix comprises a length of 25.5 Å, which fits rather well to the hydrophobic thickness of the POPC membrane (14.3 Å for one leaflet, see Table 1). From the order parameters, values for the chain extent, the hydrophobic thickness, and the area per molecules can be calculated [31] and are shown in Table 1. Further, Fig. 2B shows the chain extension plots for POPC in
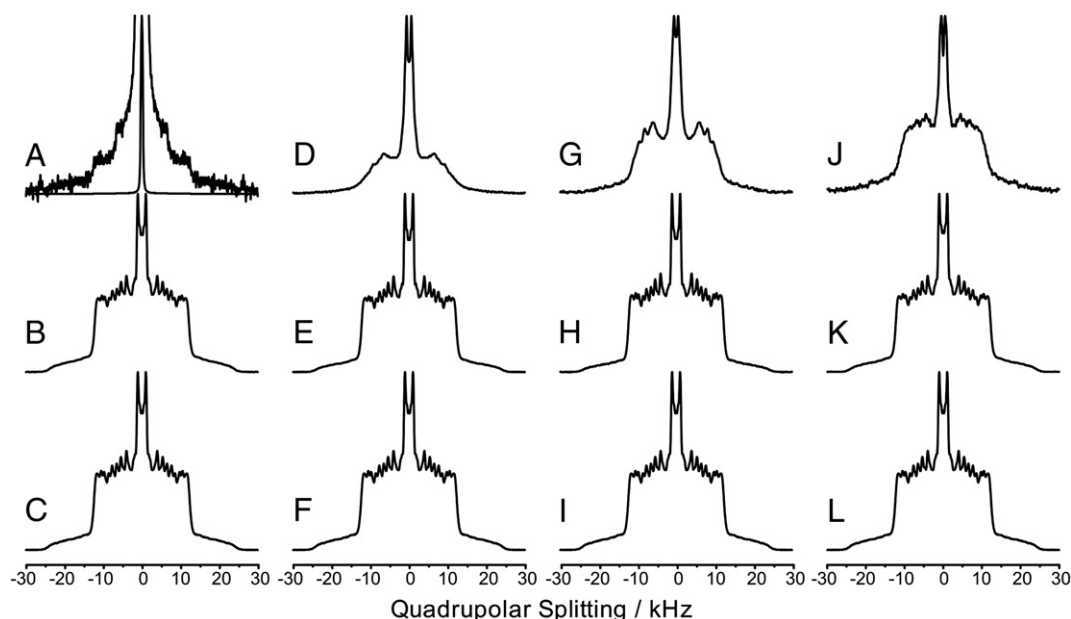

Fig. 1. Representative solid-state ^{2}H NMR spectra of deuterated peptide lipid chains of LV16ac peptides (A, D, G, and J), POPC-d_{31} in the presence of LV16ac (B, E, H, and K), and of POPC-d_{31} in the absence of LV16ac (C, F, I, and L). NMR spectra were acquired for LV16ac2 (A and B), LV16ac8 (D and E), LV16ac12 (G and H), and LV16ac16 (J and K). The peptide to lipid molar ratio was 1:30, the samples contained 50 wt.% buffer and the experiments were carried out at 37 °C. Spectra have been symmetrised for better signal to noise ratio. Spectrum (A), which is dominated by an isotropic peak, also contains two Pake doublets, which can be appreciated when the spectrum is vertically enlarged. Note that spectra (C), (F), (I), and (L) are identical but have been reproduced for better analysis of the data.
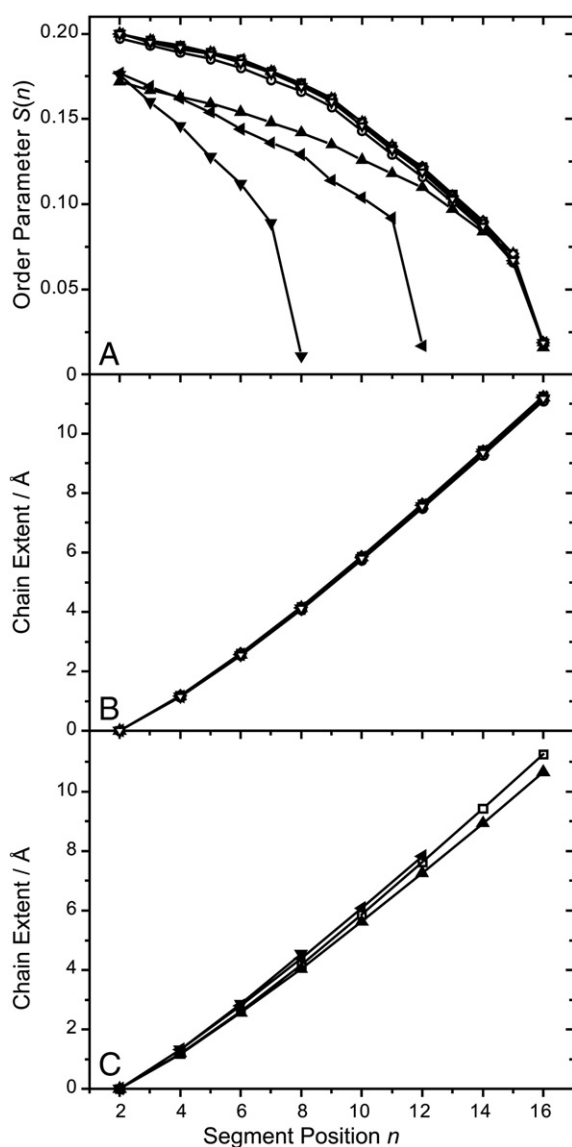
Fig. 2. Order parameter (A) and chain extents (B) as a function of chain segment n for the perdeuterated sn-1 chain of POPC in the absence and in the presence of LV16 peptides. Order parameters for the lipid modifications of the LV16 peptides are also given in panel (A, filled symbols) and the chain extent for these chains shown in panel (C). Data are shown for POPC-d_{31} (□), POPC-d_{31}/LV16 (○), POPC-d_{31}/LV16ac2 (◇), POPC-d_{31}/LV16ac8 (▽), POPC-d_{31}/LV16ac12 (◁), POPC-d_{31}/LV16ac16 (△), POPC/LV16ac8-d_{15} (▼), POPC/LV16ac12-d_{23} (◄), and POPC/LV16ac16-d_{31} (▲).

Table 1
Calculated geometric parameters: mean interfacial area (A) and volumetric hydrocarbon thickness (D_C) of one chain, chain extent (L_c^*), absolute number (n_G) and relative ratio (n_G^r) of gauche defects for the deuterated hydrocarbon chains of investigated POPC samples at 37 °C, molar ratio 30:1 for samples containing peptide. Error margins for D_C and L_c^* are ± 0.2 Å and ± 0.4 Å^2 for A [57].

	A (Å^2)	L_c^* (Å)	D_C (Å)	n_G	n_G^r (%)
POPC-d_{31}	31.0	11.3	14.3	5.9	42
POPC-d_{31}/LV16	31.2	11.1	14.2	6.1	43
POPC-d_{31}/LV16ac2	31.0	11.2	14.3	5.9	42
POPC-d_{31}/LV16ac8	31.0	11.2	14.3	6.0	43
POPC-d_{31}/LV16ac12	31.0	11.2	14.3	6.0	43
POPC-d_{31}/LV16ac16	31.0	11.2	14.3	6.0	43
POPC/LV16ac8-d_{15}	32.6	4.5	6.8	2.8	47
POPC/LV16ac12-d_{23}	32.6	7.8	10.2	4.5	45
POPC/LV16ac16-d_{31}	32.9	10.6	13.5	6.5	46

the absence and in the presence of LV16ac, which are virtually indistinguishable, suggesting that the host membrane is not influenced by LV16ac. These results can be confirmed in the measured static ^{31}P NMR spectra (data not shown), which exhibit the typical line shape for lamellar liquid crystalline phase. In these spectra, the same chemical shift anisotropy is measured for the phosphate group of POPC in the absence and in the presence of LV16ac; there is no influence of peptide on the lipid headgroup orientation or mobility.

A different picture arises for the lipid modifications on the LV16ac peptide. Order parameter plots for the lipid modifications of LV16ac are also shown in Fig. 2A (filled symbols). Independent of the lengths of the peptide lipid chains, almost identical order parameters are measured for carbon C2; however, this value is significantly lower than for the C2 position of the host membrane. Depending on the chain lengths, the order parameter plots decrease more or less steeply towards the methyl end, where again rather similar order parameters are measured. While the low order parameters at the chain end just indicate the high mobility of the lower part of the chain, the similar order of the C2 position is most likely related to the geometry of the covalent attachment of the lipid chain to the peptide's N-terminus. Altogether, these low order parameters indicate a large extent of structural and motional disorder.

From the order parameter plots, one can already conclude that there is no adaptation of the peptide lipid modifications to the structure and dynamics of the phospholipid chains. Again, the mean torque model [31] was used to determine the geometrical parameters of the lipid modifications and chain extent, hydrophobic thickness, and area per lipid chain are given in Table 1. In addition, Fig. 2C reports the chain extension plots for the lipid modifications. It is interesting to note that while not extending to the same length, the peptide lipid chains express the same slopes in the chain extension plots as the host membrane.

The LV16ac peptide lipid chains show lengths between 4.5 Å (for C8) and 10.6 Å (for C16), which are in all cases shorter than the host membrane (11.2 Å, see Table 1). Apparently, a chain length adaptation to that of the host membrane is not achieved in this system, but has been observed for other lipid-modified proteins [25–28,36,37]. In principle, both the C16 and the C12 chain could match the length of the host membrane; the C8 chain would be too short even if all bonds were in trans conformation. Instead, we observe that each peptide lipid chain shows a defined length that is related to the number of gauche conformers in the chain (between 2.8 for C8 and 6.5 for C16). However, it is interesting to note that the fraction (or percentage) of gauche conformers per chain is astonishingly similar in all lipid chains, both in phospholipids and in the peptide lipid chains.

It should be pointed out that these chain conformations are by no means static but rather a matter of intense dynamics. It is well known that trans-gauche isomerization takes place with rather short correlation times in the picosecond time window [38,39]. We also measured ^{2}H Zeeman order longitudinal relaxation rates for the phospholipid and peptide lipid chains. Here, we focus on a qualitative comparison of the chain mobility between the phospholipid and the peptide chains. To this end, the correlation of the Zeeman order relaxation rate R_{1Z} with the square of the segmental order parameter S^2 has proved to be a useful qualitative tool [40]. For saturated phospholipid membranes, these plots exhibit a linear dependence with a specific positive slope. Variations in the lipid chain dynamics alter these square law plots. For instance, the addition of cholesterol to saturated membranes increases the lipid chain order by decreasing the amplitude of the order fluctuations [26,41,42]. In the square law plot, this is expressed by a shallower slope of the linear curve. In contrast, soft membranes that are characterized by larger amplitude fluctuations, for instance mixtures of saturated phospholipids and detergents, exhibit square law plots with increased slope, which usually also provide a characteristic curved shape [26,43].

The square law plots obtained for the lipid chains of the LV16ac peptides and surrounding POPC molecules are shown in Fig. 3. As
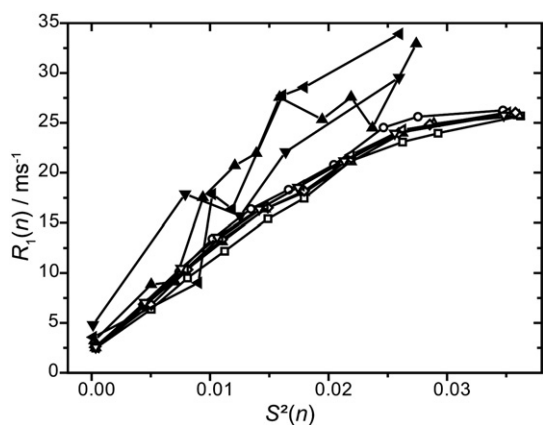
Fig. 3. Plot of the Zeeman order spin-lattice relaxation rates $R_1(n)$ versus the square of the order parameter for the perdeuterated sn-1 chain of POPC in the absence and in the presence of LV16 peptides and the lipid modification of the LV16 peptides obtained at 115.1 MHz. Data are shown for POPC-d_{31} ($\square$), POPC-d_{31}/LV16 ($\bigcirc$), POPC-d_{31}/LV16ac2 ($\diamond$), POPC-d_{31}/LV16ac8 ($\triangledown$), POPC-d_{31}/LV16ac12 ($\triangleleft$), POPC-d_{31}/LV16ac16 ($\triangle$), POPC/LV16ac8-d_{15} ($\blacktriangledown$), POPC/LV16ac12-d_{23} ($\blacktriangleleft$), and POPC/LV16ac16-d_{31} ($\blacktriangle$).

anticipated, the plots for POPC-d_{31} in the absence and in the presence of LV16ac are nearly identical and exhibit a slightly bent shape, in accordance with literature [44,45]. The acyl chains of the lipid chains of LV16ac in POPC show a similar square law plot, but the slope of the curve is increased compared to POPC. This indicates that the motions of the peptide lipid chains have slightly larger amplitudes.

3.2. LV16ac in DLPC membranes

To investigate if chain length adaptation of the peptide lipid chains occurs when the transmembrane LV16 peptides are reconstituted into thinner membranes, we studied a series of peptides in DLPC. The disaturated C12 chain phospholipid DLPC has a much smaller hydrophobic thickness of 10.9 Å for one membrane leaflet as compared to the 14.3 Å of POPC as determined in our study. The study was restricted to peptides with lipid chains long enough to match the surrounding membrane thickness, i.e. LV16ac12 and LV16ac16. Again, samples of (*i*) pure DLPC-d_{46}, (*ii*) DLPC-d_{46} with either LV16ac12 or LV16ac16, and (*iii*) DLPC containing either LV16ac12-d_{23} or LV16ac16-d_{31} were prepared and subjected to NMR analysis. ^{31}P NMR spectra of all samples confirm that all peptide containing membranes are in the lamellar liquid crystalline phase state (spectra not shown). As expected, all ^{2}H NMR spectra show the typical well resolved powder patterns with the usual superposition of Pake doublets (spectra not shown).

Fig. 4A reports the order parameters for all samples of this batch of samples. The DLPC order parameters in the absence and in the presence of LV16ac peptides are rather similar, only small deviations are observed in the upper chain region. As the hydrophobic length of the α-helix slightly exceeds the hydrophobic thickness of the membrane, we observe a small increase in the hydrophobic thickness of the membrane in the presence of the α-helical peptides.

But very interestingly, the LV16ac12 peptide, i.e. the one with the chain length that matches that of the host membrane, already shows a higher chain order. This effect is more pronounced with LV16ac16. As in the POPC matrix, the order parameters of the peptide lipid chains are identical for the upper carbon segments on both chains. Also in accordance with the results for the POPC membrane, the chain extension plots (Fig. 4B) show the same slopes for all lipid chains. However, the chain extents of the peptide lipid chains for the C16 chain of LV16ac are larger than the phospholipid chains of the DLPC host membrane, which is a logical consequence of the higher chain order. Table 2 reports all geometric data for these chains. Most strikingly, the peptide lipid modifications are now longer than the
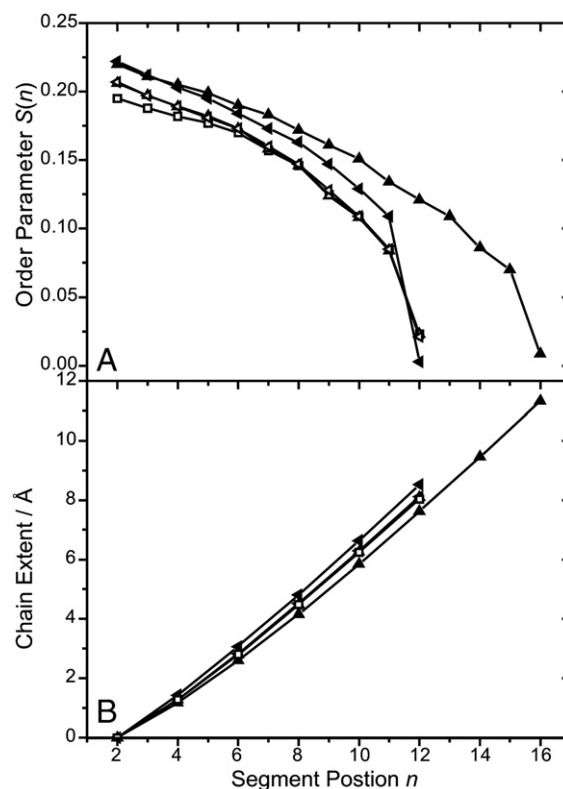

Fig. 4. Order parameter S (A) and chain extent (B) as a function of the chain segment n. Data are shown for DLPC-d_{46} ($\square$), DLPC-d_{46}/LV16ac12 ($\triangleleft$), DLPC-d_{46}/LV16ac16 ($\triangle$), DLPC/LV16ac12-d_{23} ($\blacktriangleleft$), and DLPC/LV16ac16-d_{31} ($\blacktriangle$). All LV16 containing samples were prepared at a molar ratio of 30:1.

chains of the host membrane. While for the C12 chain, only a negligible difference is seen (0.4 Å), the C16 chain of LVac16 is 3.2 Å longer than the lauroyl chains of the DLPC host membrane. This suggests a somewhat unusual chain geometry since it is unlikely that the chain would protrude into the other membrane leaflet or be exposed to the aqueous environment. Nevertheless, similar to the situation in POPC membranes, we find again that all lipid chains, both on the phospholipid and on the peptide, exhibit a similar fraction of gauche defects. For all lipid chains investigated in this study, the percentage of gauche conformers in the chains is $(42.9 \pm 0.6)\%$.

4.
Discussion

The main goal of this study was to investigate the biophysical properties of the lipid chain modifications of transmembrane α-helical peptides. To this end, *de novo* designed transmembrane peptides were covalently linked to saturated lipid chains of varying lengths. Depending on their structural flexibility according to the Leu/Val ratio and distribution, LV peptides represent a minimum

Table 2
Calculated geometric parameters: mean interfacial area (A) and volumetric hydrocarbon thickness (D_C) of one chain, chain extent (L_c^*), absolute number (n_G) and relative ratio (n_G^r) of gauche defects for the deuterated hydrocarbon chains of investigated DLPC samples at 37 °C, molar ratio 30:1. Error margins for D_C and L_c^* are ± 0.2 Å and ± 0.4 Å^2 for A [57].

	A (Å^2)	L_c^* (Å)	D_C (Å)	n_G	n_G^r (%)
DLPC-d_{46}	30.6	8.0	10.6	4.2	42.3
DLPC-d_{46}/LV16ac12	31.3	8.1	10.9	4.2	41.6
DLPC-d_{46}/LV16ac16	30.7	8.1	10.8	4.2	41.9
DLPC /LV16ac12-d_{23}	29.8	8.5	11.2	3.8	38.0
DLPC /LV16ac16-d_{31}	29.9	11.3	14.8	5.9	41.9

structural prerequisite for driving membrane fusion [4]. Such lipid modifications are found in many proteins that are involved in the biological membrane fusion and former studies have reported an influence of the N-terminal acylation on fusogenicity of LV peptides [18,19].

4.1. Insertion of lipid chains

First, we investigated if the N-terminal peptide lipid chains were inserted into the membrane. Several groups have addressed the question of protein-bound lipid chain insertion into bilayers [13,24]. All these studies agree that each methylene group that partitions into a lipid membrane contributes -3.45 kJ/mol to the binding of free energy. However, there is also an entropy penalty associated with the loss of degrees of freedom of the lipid chain. This is expressed by the well known Tanford formula derived for the partitioning of free fatty acids between n-heptane and an aqueous phase, $\Delta G^0 = (17.81 - 3.45 n_C)$ kJ/mol [46]. The 17.81 kJ/mol term represents the entropy penalty and n_C is the number of carbons in the chain. Clearly, the free energy of transferring a lipid chain from the aqueous environment to the membrane follows a linear behavior. Experimental studies on acylated peptides have confirmed the slope of -3.45 kJ/mol per inserted CH_2 segment. The energy penalty found in these experimental studies was in the order of 14 kJ/mol [13,24].

The ΔG^0 for the insertion of peptide-bound lipid chains is shown in Fig. 5 (using 14 kJ/mol entropy penalty) and should become favorable for chains of about 4–5 carbons. The entropy penalty for insertion of a lipid chain bound to a transmembrane α-helix may be different from the peptides studied so far; therefore, the gray bar represents a ± 5 kJ/mol uncertainty. This may lead to effective partitioning of slightly shorter chains as well. However, from our experimental data it is clear that the C2 chain does not partition into the lipid membrane to any significant degree.

At the typical lipid concentration of biophysical experiments of 0.2 mM, a ΔG^0 of -31.6 kJ/mol would be required for the insertion of 50% of the protein lipid chain (dotted line in Fig. 5); this is only fulfilled for the C16 chain. In our case, the lipid concentration was much higher because the water volume was restricted to 50 wt.%, which corresponds to approximately 1.2 M. For such a lipid concentration, a ΔG^0 of -9.7 kJ/mol would be sufficient to have 50% of the chains inserted into the membrane. According to this estimate, only the C8, C12, and C16 chains would be inserted, but not the C2 chain. In our experiments, we observed that indeed just the C2 chain was not inserted, all the other lipid chains showed anisotropic line shapes only, which suggested that these chains were fully inserted into the membrane. However, considering the free energy for chain
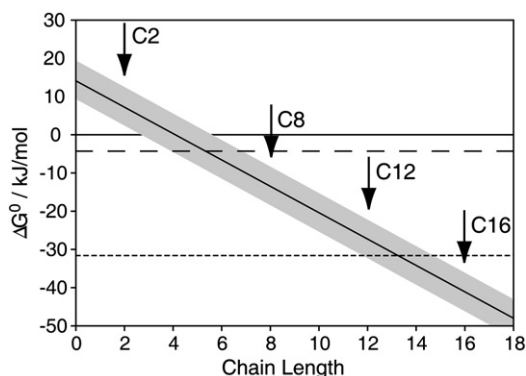
partitioning, the NMR spectrum for the C8 chain should contain about 14% isotropic signal, which was not observed. This means that it is not the total lipid concentration that is relevant for the membrane insertion, but only the local lipid concentration experienced by the peptide-bound lipid chain. Since the peptide helix is inserted into the membrane [7], the N-terminal lipid chain can only move in a very small water volume, where the lipid concentration is given by the number of lipids that are contained within the circumcircle of the peptide. Thus, a local lipid concentration in the order of 10 M and larger can be estimated depending on the lengths of the peptide lipid chains. For a local lipid concentration of 10 M, the free energy that is required to insert 50% of the lipid chains is only $\Delta G^0 = -4.3$ kJ/mol (dashed line in Fig. 5), which means that the C8, C12, and C16 chains are fully membrane embedded and only the C2 chain is not.

This simple estimation not only explains the lipid chain insertion data of the current study, it also has two important biological consequences: First, it is not the absolute but the local lipid concentration that is relevant for chain partitioning of lipid-modified proteins. In other words, when a lipid-modified protein binds to the membrane by electrostatic or hydrophobic mechanisms, even a single and relatively short lipid chain will fully insert into the bilayer, as the local lipid concentration is then much increased. Thus, also short peptide-bound C12 or C14 lipid chains that are not considered to provide sufficient hydrophobic free energy for membrane partitioning by themselves would be fully inserted, as has been observed experimentally [36,37]. Second, it should be noted that the lipid concentration within a biological cell will easily reach the mM range, if only the lipids of the plasma membrane are taken into account. Considering that the plasma membrane only contributes about 10% of all cellular lipids, the lipid concentration within a cell is in the order of 10 mM or more. This means that the C12 and C14 lipid modifications near transmembrane domains are clearly inserted in the membranes of a biological cell to provide a stable membrane anchor.

4.2. Acyl chain structure of LV16ac in POPC and DLPC

^2H NMR measurements allow determining the geometric as well as the dynamic parameters of lipid chains with great precision [31]. Most intriguingly, our measurements could determine the lengths of the peptide lipid chains in comparison to the chains of the surrounding phospholipids in the bilayer. In the membrane, the chain length and area per lipid chain are determined by the fraction of gauche conformers that are formed in a specific chain. Compared to the all trans chain, each gauche defect reduces the length of the projected chain by slightly different amounts depending on the orientation of virtual bond vector [47]. Therefore, instead of the maximum chain lengths possible of 7.6, 12.7, and 17.8 Å for the all trans chains, we measured reduced lengths of 4.5, 7.8, and 10.8 Å for the C12, C14, and C16 peptide lipid chains of LV16ac in POPC, respectively. This is shorter than the POPC palmitoyl chain length of the host membrane, which was 11.2 Å. This means that no adaptation of the peptide lipid chains to the lengths of the saturated chains of the surrounding host membrane occurs. Such chain length adaptation has been observed for Ras peptides in literature [28].

Clearly, for the transmembrane peptide lipid chains are systematically shorter than the surrounding palmitoyl chains of the phospholipid matrix. To challenge the system, we used a much thinner host membrane (DLPC) to see if length adaptation takes place in this situation in order to avoid unfavorable exposure of hydrophobic segments to the aqueous environment. In DLPC, the peptide lipid chains were a bit longer than those of the surrounding membrane, which corresponds to some rather significant mismatch of up to a few methylene segments. This may also be favorable as the saturated DLPC matrix is more ordered than the unsaturated POPC membrane, which provides more motional freedom for the peptide acyl chains. However, in interesting accordance with the results for POPC, the

Fig. 5. Plot of the free energy of transferring a lipid chain from the aqueous environment to the membrane as a function of the chain length. The gray bar symbolizes a ± 5 kJ/mol uncertainty that is added since the exact entropy penalty of chain insertion is not known. The dotted and dashed lines correspond to the energy that is required to insert 50% of a lipid chain into the membrane at a lipid concentration of 0.2 mM and 10 M, respectively; the latter corresponds to the local lipid concentration in our experiments.

percentages of gauche isomers in the peptide-bound as well as phospholipid chains are again very close to each other.

Several studies have dealt with the structure and dynamics of protein-bound lipid chains. Most detailed knowledge has been acquired for the human N-Ras protein [25–27,48], for which the lipid modifications have been shown to exactly match the thickness of the host membrane. Thereby, the C16 chain of Ras may vary its length between 8.7 and 15.5 Å [28]. Similarly, the lipid chains of GCAP-2 [36,49] have been reported to exactly match the thickness of the surrounding membrane leaflet. However, in other systems, for instance the Src protein, the lipid chain may actually exceed the thickness of the membrane leaflet [50]. This comes about when the peptide backbone at the site of lipidation is not inserted into the lipid water interface of the membrane but rather localized above the membrane surface due to Born repulsion of the polar peptide from the membrane surface of low dielectric constant.

Another interesting system to compare our data with is the C-terminal palmitoylated gramicidin A [51]. In accordance with our data, the authors observed lower order parameters for the peptide lipid chain compared to the surrounding membrane. While the lower segments of the peptide chain followed the lipid matrix, for the upper part large deviations were measured, suggesting an altered structure for the upper chain segments. One can speculate that the distinct structure and dynamics of the peptide lipid modifications are dominated by the covalent attachment to the peptide and interactions with the helical segments of the peptide. Thus, the lipid chain modifications could stabilize the α-helical transmembrane helix and decrease its motions within the bilayer, which could reduce the fusogenicity of the respective transmembrane segments. The effect of covalently attached lipid chains for the stabilization of helical structures is well known for instance for SP-C [52]. This could indicate that the intramolecular lipid-protein interactions could play an important part in the stabilization of membrane-inserted protein segments for the role of these moieties in biological functions, for instance membrane fusion. Because the peptide lipid chain is linked to the α-helical segment, it is constrained to lie in the vicinity of the peptide. The order parameters, thus, partially reflect molecular organization in the "boundary" layer of phospholipid around the peptide. This may somewhat differ from the acyl chains of a phospholipid.

All together, these data from literature along with the results from the current study suggests that a protein-bound lipid chain may or may not adapt to the hydrophobic thickness of the surrounding membrane. In general, the conformation of a given hydrocarbon chain, which determines its length and thus whether or not it matches the length of the surrounding membrane, is determined by a minimum of free energy, which has contributions from both enthalpy and entropy. A peptide lipid chain that matches the length of the surrounding lipid membrane should have optimal interactions with the surrounding membrane, thereby avoiding unfavorable water contacts, which optimizes the hydrophobic effect. Furthermore, factors such as the local chain conformation, but also the surrounding lipid-induced contributions, have to be considered for the lowest free energy. For the lipid chains attached to the N-terminus of the transmembrane LV16 peptides, we note that hydrophobic mismatches and imperfect length adaptation are tolerated, but the fraction of gauche defects remains constant in all samples. This means that an important free energy contribution must arise from the chain configurational entropy.

The relative amount of gauche conformers in a phospholipid chain is dependent on temperature, but also varies for saturated and unsaturated lipids. For DLPC and DMPC, a fraction of 39% and 35% gauche , respectively, has been reported at 30 °C [31,53]. At higher temperatures (65 °C), where also longer chains can be studied, values of 48%, 45%, 43%, and 42% are reported for DLPC, DMPC, DPPC, and DSPC, respectively. If unsaturated sn-2 chains are introduced,

relatively constant values (33–37%) can be calculated for a series of unsaturated lipids with 18:0 sn-1 chains [54]. Also, a series of lipids with 12:0, 14:0, 16:0, and 18:0 chains in sn-1 and polyunsaturated docosahexaenoic acid (22:6) in the sn-2 chain revealed very constant values around 43% at 30 °C although the order parameters were rather different [55]. This means that although the peptide lipid chains of LV16 do not adapt to the length of the host membrane, they somehow respond to the properties of the host membranes by showing a similar fraction of gauche defects within a matrix of DLPC whose chains have also fewer gauche defects than the palmitoyl chain within POPC. Thus, the peptide-linked acyl chains exhibit decreased entropy in DLPC, which can be explained by enthalpic gains when they interact with the more ordered, completely saturated DLPC bilayer. This may have interesting implications for binding acylated proteins to lipid rafts. A variety of peripheral membrane proteins have been shown to bind to rafts by way of covalently linked acyl chains [56].

In summary, our results show that N-terminal lipid modifications of transmembrane α-helices are membrane-inserted except for very short chains. According to our measurements, even a C8 lipid chain is sufficient to insert into the membrane. This is a simple consequence of the partitioning of those chains from water into a membrane environment that depends upon the local lipid concentration. In contrast to other results, the peptide lipid modifications do not show a chain length adaptation to the host membrane and show order parameters that are not related to those of the host membrane. Further, there is no influence of the lipidated peptides onto the structure and packing properties of the host membrane, which is most likely related to the fact that no hydrophobic mismatch between the transmembrane helix and the host membrane occurs.

Acknowledgements

References

[1] R. Jahn, R.H. Scheller, SNAREs–engines for membrane fusion, Nat. Rev. Mol. Cell Biol. 7 (2006) 631–643.

[2] D. Langosch, M. Hofmann, C. Ungermann, The role of transmembrane domains in membrane fusion, Cell Mol. Life Sci. 64 (2007) 850–864.

[3] A. Lorin, B. Charloteaux, Y. Fridmann-Sirkis, A. Thomas, Y. Shai, R. Brasseur, Mode of membrane interaction and fusogenic properties of a de novo transmembrane model peptide depend on the length of the hydrophobic core, J. Biol. Chem. 282 (2007) 18388–18396.

[4] M.W. Hofmann, K. Weise, J. Ollesch, P. Agrawal, H. Stalz, W. Stelzer, F. Hulsbergen, H. de Groot, K. Gerwert, J. Reed, D. Langosch, De novo design of conformationally flexible transmembrane peptides driving membrane fusion, Proc. Natl. Acad. Sci. U. S. A. 101 (2004) 14776–14781.

[5] D.Z. Cleverley, J. Lenard, The transmembrane domain in viral fusion: essential role for a conserved glycine residue in vesicular stomatitis virus G protein, Proc. Natl. Acad. Sci. U. S. A. 95 (1998) 3425–3430.

[6] D. Langosch, J.M. Crane, B. Brosig, A. Hellwig, L.K. Tamm, J. Reed, Peptide mimics of SNARE transmembrane segments drive membrane fusion depending on their conformational plasticity, J. Mol. Biol. 311 (2001) 709–721.

[7] J. Ollesch, B.C. Poschner, J. Nikolaus, M.W. Hofmann, A. Herrmann, K. Gerwert, D. Langosch, Secondary structure and distribution of fusogenic LV-peptides in lipid membranes, Eur. Biophys. J. 37 (2008) 435–445.

[8] M.W. Hofmann, B.C. Poschner, S. Hauser, D. Langosch, pH-Activated fusogenic transmembrane LV-peptides, Biochemistry 46 (2007) 4204–4209.

[9] P. Agrawal, S. Kiihne, J. Hollander, M. Hofmann, D. Langosch, H. de Groot, A solid-state NMR study of changes in lipid phase induced by membrane-fusogenic LV-peptides, Biochim. Biophys. Acta. 1798 (2010) 202–209.

[10] A. Couve, V. Protopopov, J.E. Gerst, Yeast synaptobrevin homologs are modified posttranslationally by the addition of palmitate, Proc. Natl. Acad. Sci. U. S. A. 92 (1995) 5987–5991.

[11] J. Valdez-Taubas, H. Pelham, Swf1-dependent palmitoylation of the SNARE Tlg1 prevents its ubiquitination and degradation, EMBO J. 24 (2005) 2524–2532.

[12] L. Brunsveld, H. Waldmann, D. Huster, Membrane binding of lipidated Ras peptides and proteins—the structural point of view, Biochim. Biophys. Acta 1788 (2009) 273–288.

[13] R.M. Peitzsch, S. McLaughlin, Binding of acylated peptides and fatty acids to phospholipid vesicles: pertinence to myristoylated proteins, Biochemistry 32 (1993) 10436–10443.

[14] S. Shahinian, J.R. Silvius, Doubly-lipid-modified protein sequence motifs exhibit long-lived anchorage to lipid bilayer membranes, Biochemistry 34 (1995) 3813–3822.

[15] Y.G. Smirnova, S.J. Marrink, R. Lipowsky, V. Knecht, Solvent-exposed tails as prestalk transition states for membrane fusion at low hydration, J. Am. Chem. Soc. 132 (2010) 6710–6718.

[16] D. Huster, K. Arnold, K. Gawrisch, Investigation of lipid organization in biological membranes by two-dimensional nuclear Overhauser enhancement spectroscopy, J. Phys. Chem. B 103 (1999) 243–251.

[17] D. Huster, K. Gawrisch, NOESY NMR crosspeaks between lipid headgroups and hydrocarbon chains: spin diffusion or molecular disorder? J. Am. Chem. Soc. 121 (1999) 1992–1993.

[18] B.C. Poschner, K. Fischer, J.R. Herrmann, M.W. Hofmann, D. Langosch, Structural features of fusogenic model transmembrane domains that differentially regulate inner and outer leaflet mixing in membrane fusion, Mol. Membr. Biol. 27 (2010) 1–11.

[19] B.C. Poschner, D. Langosch, Stabilization of conformationally dynamic helices by covalently attached acyl chains, Protein Sci. 18 (2009) 1801–1805.

[20] T. Sakai, R. Ohuchi, M. Ohuchi, Fatty acids on the A/USSR/77 influenza virus hemagglutinin facilitate the transition from hemifusion to fusion pore formation, J. Virol. 76 (2002) 4603–4611.

[21] R. Wagner, A. Herwig, N. Azzouz, H.D. Klenk, Acylation-mediated membrane anchoring of avian influenza virus hemagglutinin is essential for fusion pore formation and virus infectivity, J. Virol. 79 (2005) 6449–6458.

[22] C. Fischer, B. Schroth-Diez, A. Herrmann, W. Garten, H.D. Klenk, Acylation of the influenza hemagglutinin modulates fusion activity, Virology 248 (1998) 284–294.

[23] G.B. Melikyan, H. Jin, R.A. Lamb, F.S. Cohen, The role of the cytoplasmic tail region of influenza virus hemagglutinin in formation and growth of fusion pores, Virology 235 (1997) 118–128.

[24] C.T. Pool, T.E. Thompson, Chain length and temperature dependence of the reversible association of model acylated proteins with lipid bilayers, Biochemistry 37 (1998) 10246–10255.

[25] D. Huster, A. Vogel, C. Katzka, H.A. Scheidt, H. Binder, S. Dante, T. Gutberlet, O. Zschörnig, H. Waldmann, K. Arnold, Membrane insertion of a lipidated ras peptide studied by FTIR, solid-state NMR, and neutron diffraction spectroscopy, J. Am. Chem. Soc. 125 (2003) 4070–4079.

[26] A. Vogel, C.P. Katzka, H. Waldmann, K. Arnold, M.F. Brown, D. Huster, Lipid modifications of a ras peptide exhibit altered packing and mobility versus host membrane as detected by ^{2}H solid-state NMR, J. Am. Chem. Soc. 127 (2005) 12263–12272.

[27] A. Vogel, K.-T. Tan, H. Waldmann, S.E. Feller, M.F. Brown, D. Huster, Flexibility of ras lipid modifications studied by ^{2}H solid-state NMR and molecular dynamics simulations, Biophys. J. 93 (2007) 2697–2712.

[28] A. Vogel, G. Reuther, K. Weise, G. Triola, J. Nikolaus, K.T. Tan, C. Nowak, A. Herrmann, H. Waldmann, R. Winter, D. Huster, The lipid modifications of Ras that sense membrane environments and induce local enrichment, Angew. Chem. Int. Ed Engl. 48 (2009) 8784–8787.

[29] J.H. Davis, Deuterium magnetic resonance study of the gel and liquid crystalline phases of dipalmitoyl phosphocholine, Biophys. J. 27 (1979) 339–358.

[30] J. Seelig, Deuterium magnetic resonance: theory and application to lipid membranes, Q. Rev. Biophys. 10 (1977) 353–418.

[31] H.I. Petrache, S.W. Dodd, M.F. Brown, Area per lipid and acyl length distributions in fluid phosphatidylcholines determined by ^{2}H NMR spectroscopy, Biophys. J. 79 (2000) 3172–3192.

[32] M.F. Brown, Membrane structure and dynamics studied with NMR spectroscopy, in: K.M. Merz, B. Roux (Eds.), Biological membranes. A molecular perspective from computation and experiment, Birkhäuser, Boston, 1996, pp. 175–252.

[33] J.H. Davis, K.R. Jeffrey, M. Bloom, M.I. Valic, T.P. Higgs, Quadrupolar echo deuteron magnetic resonance spectroscopy in ordered hydrocarbon chains, Chem. Phys. Lett. 42 (1976) 390–394.

[34] M.A. McCabe, S.R. Wassall, Fast-Fourier-transform DePaking, J. Magn. Reson. B 106 (1995) 80–82.

[35] S.E. Feller, K. Gawrisch, A.D. MacKerell Jr., Polyunsaturated fatty acids in lipid bilayers: intrinsic and environmental contributions to their unique physical properties, J. Am. Chem. Soc. 124 (2002) 318–326.

[36] A. Vogel, T. Schroder, C. Lange, D. Huster, Characterization of the myristoyl lipid modification of membrane-bound GCAP-2 by H-2 solid-state NMR spectroscopy, Biochim. Biophys. Acta 1768 (2007) 3171–3181.

[37] S. Theisgen, H.A. Scheidt, A. Magalhaes, T.J. Bonagamba, D. Huster, A solid-state NMR study of the structure and dynamics of the myristoylated N-terminus of the guanylate cyclase-activating protein-2, Biochim. Biophys. Acta. 1798 (2010) 266–274.

[38] S.E. Feller, D. Huster, K. Gawrisch, Interpretation of NOESY cross-relaxation rates from molecular dynamics simulations of a lipid bilayer, J. Am. Chem. Soc. 121 (1999) 8963–8964.

[39] T.P. Trouard, T.M. Alam, M.F. Brown, Angular dependence of deuterium spin-lattice relaxation rates of macroscopically oriented dilauroylphosphatidylcholine in the liquid-crystalline state, J. Chem. Phys. 101 (1994) 5229–5261.

[40] M.F. Brown, Theory of spin-lattice relaxation in lipid bilayers and biological membranes. ^{2}H and ^{14}N quadrupolar relaxation, J. Chem. Phys. 77 (1982) 1576–1799.

[41] K. Rajamoorthi, H.I. Petrache, T.J. McIntosh, M.F. Brown, Packing and viscoelasticity of polyunsaturated omega-3 and omega-6 lipid bilayers as seen by ^{2}H NMR and X-ray diffraction, J. Am. Chem. Soc. 127 (2005) 1576–1588.

[42] M.F. Brown, R.L. Thurmond, S.W. Dodd, D. Otten, K. Beyer, Composite membrane deformation on the mesoscopic length scale, Phys. Rev. E. 64 (2001) 010901.

[43] M.F. Brown, R.L. Thurmond, S.W. Dodd, D. Otten, K. Beyer, Elastic deformation of membrane bilayers probed by deuterium NMR relaxation, J. Am. Chem. Soc. 124 (2002) 8471–8484.

[44] O. Kaczmarek, N. Brodersen, A. Bunge, L. Loser, D. Huster, A. Herrmann, A. Arbuzova, J. Liebscher, Synthesis of nucleosides with 2 '-fixed lipid anchors and their behavior in phospholipid membranes, Eur. J. Org. Chem. (2008) 1917–1928.

[45] A. Bunge, M. Loew, P. Pescador, A. Arbuzova, N. Brodersen, J. Kang, L. Dahne, J. Liebscher, A. Herrmann, G. Stengel, D. Huster, Lipid membranes carrying lipophilic cholesterol-based oligonucleotides—characterization and application on layer-by-layer coated particles, J. Phys. Chem. B. 113 (2009) 16425–16434.

[46] C. Tanford, The hydrophobic effect: formation of micelles and biological membranes, John Wiley & Sons, New York, 1980.

[47] A. Salmon, S.W. Dodd, G.D. Williams, J.M. Beach, M.F. Brown, Configurational statistics of acyl chains in polyunsaturated lipid bilayers from deuterium NMR, J. Am. Chem. Soc. 109 (1987) 2600–2609.

[48] A.A. Gorfe, R. Pellarin, A. Caflisch, Membrane localization and flexibility of a lipidated ras peptide studied by molecular dynamics simulations, J. Am. Chem. Soc. 126 (2004) 15277–15286.

[49] A. Vogel, H.A. Scheidt, D. Huster, The distribution of lipid attached EPR probes in bilayers. Application to membrane protein topology, Biophys. J. 85 (2003) 1691–1701.

[50] H.A. Scheidt, D. Huster, Structure and dynamics of the myristoyl lipid modification of Src peptides determined by ^{2}H solid-state NMR spectroscopy, Biophys. J. 96 (2009) 3663–3672.

[51] T.C. Vogt, J.A. Killian, B. de Kruijff, Structure and dynamics of the acyl chain of a transmembrane polypeptide, Biochemistry 33 (1994) 2063–2070.

[52] A. Gonzales-Horta, D. Andreu, M.R. Morrow, J. Perez-Gil, Effects of palmitoylation on dynamics and phospholipid-bilayer-perturbing properties of the N-terminal segment of pulmonary surfactant protein SP-C, as revealed by ^{2}H-NMR, Biophys. J. 95 (2008) 2308–2317.

[53] J.P. Douliez, A. Leonard, E.J. Dufourc, Restatement of order parameters in biomembranes—calculation of C-C bond order parameters from C-D quadrupolar splittings, Biophys. J. 68 (1995) 1727–1739.

[54] L.L. Holte, S.A. Peter, T.M. Sinnwell, K. Gawrisch, ^{2}H nuclear magnetic resonance order parameter profiles suggest a change of molecular shape for phosphatidylcholines containing a polyunsaturated acyl chain, Biophys. J. 68 (1995) 2396–2403.

[55] H.I. Petrache, A. Salmon, M.F. Brown, Structural properties of docosahexaenoyl phospholipid bilayers investigated by solid-state ^{2}H NMR spectroscopy, J. Am. Chem. Soc. 123 (2001) 12611–12622.

[56] K. Simons, E. Ikonen, Functional rafts in cell membranes, Nature 387 (1997) 569–572.

[57] L.L. Holte, F. Separovic, K. Gawrisch, Nuclear magnetic resonance investigations of hydrocarbon chain packing in bilayers of polyunsaturated phospholipids, Lipids 31 (1996), S-199-S-203.